

Valence, spin, and orbital state of Co ions in one-dimensional $\text{Ca}_3\text{Co}_2\text{O}_6$: An x-ray absorption and magnetic circular dichroism study

T. Burnus,¹ Z. Hu,¹ M. W. Haverkort,¹ J. C. Cezar,² D. Flahaut,³ V. Hardy,⁴ A. Maignan,⁴ N. B. Brookes,² A. Tanaka,⁵ H. H. Hsieh,⁶ H.-J. Lin,⁷ C. T. Chen,⁷ and L. H. Tjeng¹

¹*II. Physikalisches Institut, Universität zu Köln, Zùlpicher Straße 77, D-50937 Köln, Germany*

²*European Synchrotron Radiation Facility, Boîte Postale 220, Grenoble 38043, France*

³*Laboratoire CRISMAT, UMR 6508, ENSICAEN/CNRS, Université de Caen, 6, Boulevard du Maréchal Juin, 14050 Caen Cedex, France*

⁴*Laboratoire CRISMAT, UMR 6508, Institut des Sciences de la Matière et du Rayonnement, Université de Caen, 6, Boulevard du Maréchal Juin, 14050 Caen Cedex, France*

⁵*Department of Quantum Matter, ADSM, Hiroshima University, Higashi-Hiroshima 739-8530, Japan*

⁶*Chung Cheng Institute of Technology, National Defense University, Taoyuan 335, Taiwan*

⁷*National Synchrotron Radiation Research Center, 101 Hsin-Ann Road, Hsinchu 30077, Taiwan*

(Received 19 June 2006; revised manuscript received 7 October 2006; published 14 December 2006)

We have investigated the valence, spin, and orbital state of the Co ions in the one-dimensional cobaltate $\text{Ca}_3\text{Co}_2\text{O}_6$ using x-ray absorption and x-ray magnetic circular dichroism at the $\text{Co-}L_{2,3}$ edges. The Co ions at both the octahedral Co_{oct} and trigonal Co_{trig} sites are found to be in a $3+$ state. From the analysis of the dichroism we established a low-spin state for the Co_{oct} and a high-spin state with an anomalously large orbital moment of $1.7\mu_B$ at the $\text{Co}_{\text{trig}}^{3+}$ ions. This large orbital moment along the c -axis chain and the unusually large magnetocrystalline anisotropy can be traced back to the double occupancy of the d_2 orbital in trigonal crystal field.

DOI: [10.1103/PhysRevB.74.245111](https://doi.org/10.1103/PhysRevB.74.245111)

PACS number(s): 71.27.+a, 71.70.Ej, 75.20.Hr, 75.30.Gw

The one-dimensional $\text{Ca}_3\text{Co}_2\text{O}_6$ has attracted great interest in recent years due to the observation of the stair-step jumps in the magnetization at regular intervals of the applied magnetic field.¹⁻⁹ The rhombohedral structure of this compound consists of $[\text{Co}_2\text{O}_6]_{\infty}$ chains running along the c axis of the hexagonal unit cell.¹⁰ In each chain, CoO_6 octahedra alternate with CoO_6 trigonal prisms. The magnetism is Ising-like and directed along the Co chains with large magnetic moments of $4.8\mu_B$ per formula unit.^{11,12} The intrachain coupling is ferromagnetic with a spin-freeze at $T_{\text{SF}}=7$ K, and the chains couple antiferromagnetically with a Néel temperature of $T_N=25$ K.¹¹

Based on density-functional-theory calculations, Vidya *et al.* claimed a low-spin (LS) $\text{Co}_{\text{oct}}^{4+}$ and a high-spin (HS) $\text{Co}_{\text{trig}}^{2+}$ state for $\text{Ca}_3\text{Co}_2\text{O}_6$.¹³ However, other experimental and theoretical works have proposed a Co^{3+} valence state at both the octahedral and trigonal Co sites, with the Co_{oct} LS ($S=0$) and the Co_{trig} HS ($S=2$) state.¹⁴⁻¹⁸ The Ising character of the magnetism is also subject of discussion. Dai and co-workers found from their band structure calculations that the spin-orbit-inactive d_0 orbital lies lowest of all Co_{trig} crystal-field levels,^{17,19} and had to invoke excited states in their attempt to explain the Ising magnetism. Wu *et al.*¹⁸ on the other hand, calculated that it is the spin-orbit-active d_2 orbital which lies lowest, giving a very different picture for the Ising magnetism.

In this paper we have applied soft-x-ray absorption spectroscopy (XAS) and magnetic circular dichroism (XMCD) at the $\text{Co-}L_{2,3}$ edges to resolve the Co valence, spin and orbital state issue in $\text{Ca}_3\text{Co}_2\text{O}_6$. We have also carried out detailed configuration-interaction cluster calculations to analyze the spectra. We found that the Co ions are all in the $3+$ state, that the Co_{oct} are nonmagnetic, and that the $\text{Co}_{\text{trig}}^{3+}$ carry a $1.7\mu_B$

orbital moment. We clarify the orbital occupation issue and the origin of the Ising magnetism.

The $\text{Ca}_3\text{Co}_2\text{O}_6$ single crystals were grown by heating a mixture of $\text{Ca}_3\text{Co}_4\text{O}_9$ and K_2CO_3 in a weight ratio of 1:7 at 950°C for 50 h in an alumina crucible in air. The cooling was performed in two steps, first down to 930°C at a rate of 10°C/h and then down to room temperature at 100°C/h .⁸ The $\text{Co-}L_{2,3}$ XAS spectra of $\text{Ca}_3\text{Co}_2\text{O}_6$ and of CoO and EuCoO_3 (Ref. 20) as references were recorded at the Dragon beamline of the National Synchrotron Radiation Research Center (NSRRC) in Taiwan with an energy resolution of 0.3 eV. The first sharp peak at 777 eV of photonenergy at the $\text{Co-}L_3$ edge of CoO was used for energy calibration, which enabled us to achieve better than 0.05 eV accuracy in the relative energy alignment. The XMCD spectra were collected at the ID08 beamline of the European Synchrotron Radiation Facility (ESRF) in Grenoble with a resolution of 0.25 eV and a degree of circular polarization close to 100% in a magnetic field of 5.5 Tesla with the sample kept at approximately 15–20 K, using a dedicated superconducting magnet setup from Oxford Instruments. The Poynting vector of the photons and the magnetic field were both parallel to the c axis. The single-domain $\text{Ca}_3\text{Co}_2\text{O}_6$ crystal used for the XMCD experiment was needle-shaped with a dimension of $0.2 \times 0.2 \times 10 \text{ mm}^3$ for $a \times b \times c$. Clean sample areas were obtained by cleaving the crystals *in situ* in chambers with base pressures in the low 10^{-10} mbar range. The $\text{Co } L_{2,3}$ spectra were recorded using the total-electron-yield method (TEY).

Figure 1 shows the $\text{Co-}L_{2,3}$ XAS spectrum of $\text{Ca}_3\text{Co}_2\text{O}_6$ together with that of CoO and EuCoO_3 . CoO serves here as a $2+$ reference and EuCoO_3 as a LS $3+$ reference.²⁰ One can see first of all that the $2+$ spectrum (CoO) contains peaks

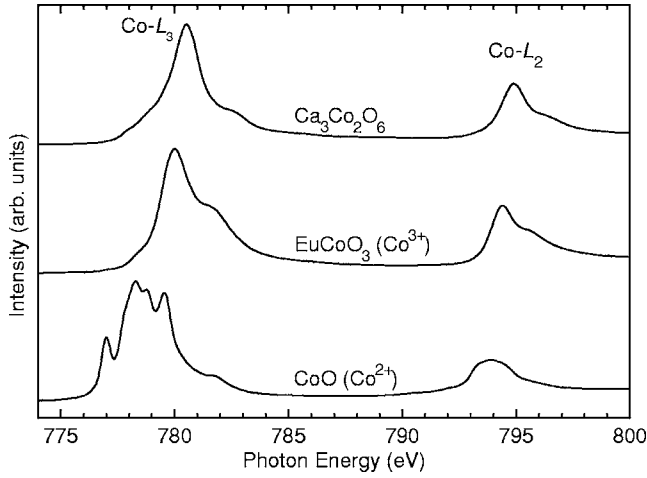


FIG. 1. Co- $L_{2,3}$ XAS spectra of $\text{Ca}_3\text{Co}_2\text{O}_6$, CoO , and EuCoO_3 .

that are 2 or more eV lower in energy than the main peak of the 3+ spectrum (EuCoO_3). It is well known that x-ray absorption spectra at the transition-metal $L_{2,3}$ edges are highly sensitive to the valence state. An increase of the valence of the metal ion by one results in a shift of the $L_{2,3}$ XAS spectra to higher energies by 1 eV or more.²¹ This shift is due to a final state effect in the x-ray absorption process. The energy difference between a $3d^n$ ($3d^7$ for Co^{2+}) and a $3d^{n-1}$ ($3d^6$ for Co^{3+}) configuration is $\Delta E = E(2p^6 3d^{n-1} \rightarrow 2p^5 3d^n) - E(2p^6 3d^n \rightarrow 2p^5 3d^{n+1}) \approx U_{pd} - U_{dd} \approx 1-2$ eV, where U_{dd} is the Coulomb repulsion energy between two $3d$ electrons and U_{pd} the one between a $3d$ electron and the $2p$ core hole.

One can observe from Fig. 1 that the $\text{Ca}_3\text{Co}_2\text{O}_6$ spectrum has no features at the low-energy side, which otherwise could have indicated the presence of Co^{2+} species as in CoO . Instead, the spectrum has a much closer resemblance to that of Co^{3+} , as in EuCoO_3 . This means that one can safely rule out the $\text{Co}^{2+}/\text{Co}^{4+}$ scenario.¹³ In other words, the XAS experiment reveals unambiguously that both the Co_{oct} and the Co_{trig} ions are in the 3+ valence state. This result supports the analysis of the Co $2p$ core-level x-ray photoemission spectra¹⁵ and band-structure calculations.^{16,18}

In order to resolve the spin-state issue, we now resort to XMCD. The top part (a) of Fig. 2 depicts Co- $L_{2,3}$ XAS spectra taken with circularly polarized light with the photon spin parallel (red solid line, μ^+) and antiparallel (black dashed line, μ^-) aligned to the magnetic field. The quantization axis z has been chosen to be parallel to the c axis, which is the easy magnetization axis.³ One can clearly observe large differences between the spectra using these two alignments. The difference spectrum, i.e., the XMCD spectrum, is also shown (blue dash-dotted line, $\mu^+ - \mu^-$). Using the well-known XMCD sum rule developed by Thole *et al.*,²²

$$L_z = \frac{4}{3} \frac{\int [\mu^+(E) - \mu^-(E)] dE}{\int [\mu^+(E) + \mu^-(E)] dE} (10 - N_e), \quad (1)$$

where N_e is the number of the Co d electrons, we can extract directly the orbital (L_z) contribution to the magnetic moment

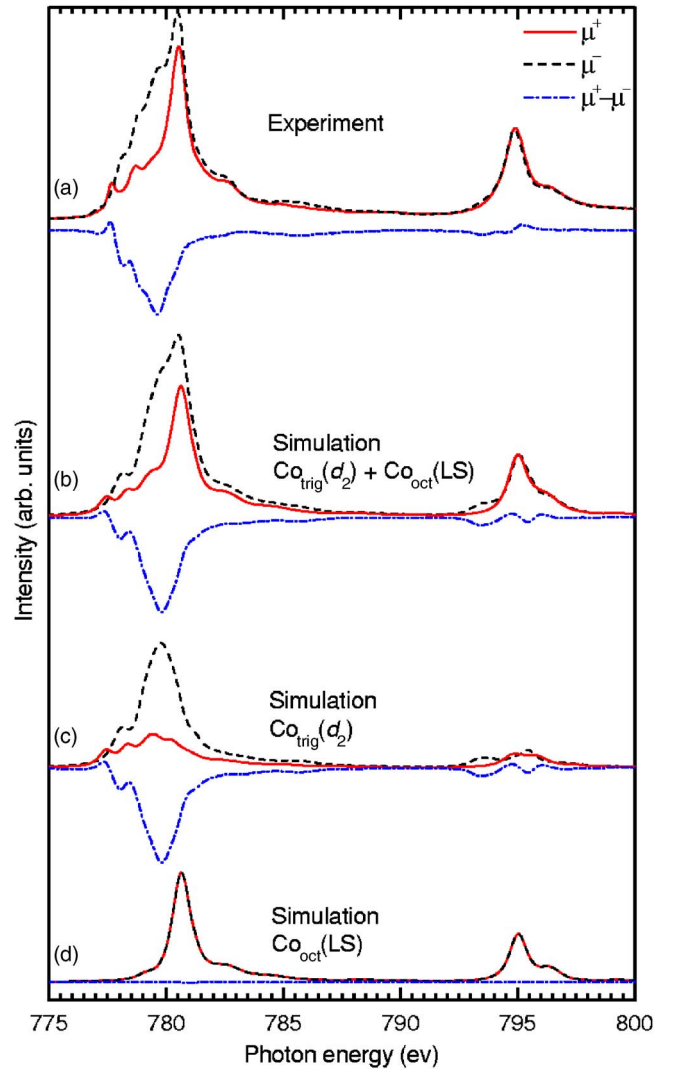


FIG. 2. (Color online) (a) Measured soft-x-ray absorption spectra with parallel (μ^+ , red solid line) and antiparallel (μ^- , black dashed line) alignment between photon spin and magnetic field, together with the difference spectrum ($\mu^+ - \mu^-$, blue dashed-dotted line). (b) Simulated sum spectra assuming a doubly occupied d_2 orbital for the Co_{trig} and low-spin (LS) Co_{oct} ions; (c) and (d) Contribution of the Co_{trig} and Co_{oct} ions to the simulated sum spectra.

without the need to do detailed modeling. Assuming an average Co $3d$ occupation number of about $N_e = 6.5$ electrons (estimated for a HS Co^{3+} oxide²³ and also to be justified below by cluster calculations) we find a value of $1.2\mu_B$ for the L_z , which is a very large number indicating that the ground state is strongly spin-orbit active.

To extract more detailed information concerning the spin and orbital states from the Co- $L_{2,3}$ XAS spectra, we have carried out simulations for the XMCD spectra using the well-proved configuration-interaction (CI) cluster model.²⁴⁻²⁶ The method uses for each Co site a CoO_6 cluster that includes the full atomic multiplet theory and the local effects of the solid. It accounts for the intra-atomic $3d-3d$ and $2p-3d$ Coulomb interactions, the atomic $2p$ and $3d$ spin-orbit couplings, the O $2p$ -Co $3d$ hybridization, and the proper local crystal-field parameters. In the configuration-interaction cluster calcula-

tion we describe the ground state by the configurations

$$\Psi = \alpha_6|d^6\rangle + \alpha_7|d^7\bar{L}\rangle + \alpha_8|d^8\bar{L}^2\rangle + \alpha_9|d^9\bar{L}^3\rangle, \quad (2)$$

where \bar{L} denotes a ligand hole and $\sum_{i=6}^9 \alpha_i^2 = 1$.^{17,28} The transition-metal electron occupation is then given by

$$N_e = 6\alpha_6^2 + 7\alpha_7^2 + 8\alpha_8^2 + 9\alpha_9^2. \quad (3)$$

The simulations have been carried out using the program XTLS 8.3.²⁴

In octahedral symmetry the $3d$ orbitals split up in the well-known e_g and t_{2g} levels; the splitting is given by $10Dq$. In a trigonal prismatic environment, however, it is found that the x^2-y^2 is degenerate with the xy , and the yz with zx orbital.^{17,18} In the presence of the spin-orbit coupling, it is then better to use the complex orbitals d_0 , d_2/d_{-2} , and d_1/d_{-1} . Band structure calculations indicate that the d_1/d_{-1} band is split off from the d_0 and d_2/d_{-2} bands by about 1 eV, while the d_0 and d_2/d_{-2} bands are almost degenerate.^{17,18} Critical for the magnetism and for the line shape of the simulated spectra are the crystal field parameter $10Dq$ for the $\text{Co}_{\text{oct}}\text{O}_6$ cluster and the crystal field parameter for the splitting between the nearly degenerate d_0 and d_2 orbitals of the $\text{Co}_{\text{trig}}\text{O}_6$ cluster. $10Dq$ needs to be critically tuned since this is set to determine whether $\text{Co}_{\text{oct}}\text{O}_6$ cluster is in the LS or HS state.²⁹ The trigonal prism crystal field has also to be fine-tuned since it determines whether the d_2 or the d_0 lies lowest, and thus the magnitude of the orbital moment and strength of the magnetocrystalline anisotropy as we will show below. Tuning of these parameters will be done by establishing which of the simulated spectra reproduce the experimentally observed ones.

As a starting point, we make the assumption that the Co_{oct} ion is in the LS state, based on the observation that the average $\text{Co}_{\text{oct}}\text{-O}$ bond length of 1.916 Å in this material¹⁰ is shorter than the 1.925 Å in LaCoO_3 at 5 K, which is known to be LS.³⁰ With such a short length, the Co ion is subjected to a large enough $10Dq$, sufficient to stabilize the nonmagnetic LS state^{29,30} for $\text{Co}_{\text{oct}}^{3+}$ ions in $\text{Ca}_3\text{Co}_2\text{O}_6$. With this starting point, the magnetism and the XMCD signal must originate from the Co_{trig} ions. This is quite plausible since with the extremely large $\text{Co}_{\text{trig}}\text{-O}$ average bond length of 2.062 Å,¹⁰ which is much larger than 1.961 Å for LaCoO_3 at 1000 K,³⁰ one can expect that the crystal field is small enough to stabilize the HS state.²⁹ Based on the observation that the orbital contribution to the magnetic moment is extremely large, we take the d_2 *ansatz* for the Co_{trig} and not the d_0 . In the CI calculation, the parameters for the multipole part of the Coulomb interactions were given by the Hartree-Fock values, while the monopole parts (U_{dd} , U_{pd}) were estimated from photoemission experiments on Co^{3+} materials.³¹ The one-electron parameters such as the O $2p$ -Co $3d$ charge-transfer energies and integrals were estimated from band-structure results.¹⁷⁻¹⁹ The charge-transfer energy is given by $\Delta = E(d^7\bar{L}) - E(d^6) = 1.5$ eV, the d - d Coulomb repulsion by $U_{dd} = 5.5$ eV and of p - d of the excited Co by $U_{pd} = 7.0$ eV; the Slater integrals have been reduced to 80% of their Hartree-Fock value. An exchange field of $H_{\text{ex}} = 3$ meV has been used. For the Co_{trig} ions the ionic crystal splittings are

$\Delta E_{d_1/d_2}^{\text{ionic}} = 0.9$ eV and $\Delta E_{d_0/d_2}^{\text{ionic}} = 0.05$ eV taken from band-structure calculation,¹⁸ the hybridization is $V_{d_1}^{\text{hyb}} = 1.88$ eV, $V_{d_0}^{\text{hyb}} = 1.28$ eV, and $V_{d_2}^{\text{hyb}} = 1.25$ eV. For Co_{oct} ions $pd\sigma = -1.44$ eV and $pd\pi = 0.63$ eV was used. With this set of parameters we have found a LS-HS transition for Co_{oct} at $10Dq = 0.65$ eV. Here we used $10Dq = 0.8$ eV, based on band-structure calculation, which is the same value as for EuCoO_3 known as a LS Co^{3+} oxide.²⁰

The results of these simulations are given by curves (b) in Fig. 2, together with a breakdown into the separate contributions of the Co_{trig} [curves (c)] and Co_{oct} [curves (d)] ions. One can clearly observe that the simulations [curves (b)] reproduce the experimental spectra quite well. All major and minor peaks in the individual experimental XAS (μ^+ , μ^-) and XMCD ($\mu^+ - \mu^-$) spectra [curves (a)] are present in the simulations [curves (b)]. It is almost needless to remark that the entire simulated XMCD signal is coming from the HS Co_{trig} ions [curves (c)], since we started with a nonmagnetic LS Co_{oct} [curves (d)]. In the simulation, we find $S_z = 1.8\mu_B$ and $L_z = 1.7\mu_B$, giving a total magnetic moment of $2S_z + L_z = 5.3\mu_B$ per formula unit. Due to strong hybridization between Co $3d$ and O $2p$, the $3d$ occupation numbers of the Co_{trig} ions and the Co_{oct} are 6.3 and 6.8, respectively, giving on average 6.5 electrons as used for the sum rules. The calculated total moment from the simulation compares reasonably well with the $4.8\mu_B$ value from direct magnetization measurements.^{6,12} Yet, the simulated L_z value ($1.7\mu_B$) is appreciably larger than the one derived from the experiment using the XMCD sum rule ($1.2\mu_B$). However, looking more closely at the simulated and experimental XMCD spectra, we can clearly see that the XMCD spectra have very similar line shapes and that the distinction is mainly in the amplitude, i.e., a matter of scaling. This indicates that the discrepancy in the L_z determination might be caused by the fact that the sample is not fully magnetized in our experiment. According to magnetization measurements one can only achieve 90% of the saturation magnetization at 5.5 T.¹² In addition, slight misalignment of the sample together with the high magnetocrystalline anisotropy may account for some further reduction of the experimental value.

Having established that the d_2/LS scenario for the $\text{Co}_{\text{trig}}/\text{Co}_{\text{oct}}$ ions explains well the experimental spectra, we now investigate the sensitivity of our analysis. For this we change the *ansatz* for the Co_{trig} ion: we now set the d_0 orbital to be energetically lower than the d_2 .³² The result is shown in Fig. 3, in which the simulated XMCD spectrum (b) is compared with the experimental one (a). One can unambiguously recognize large discrepancies in the line shapes, not only in the L_3 region (777–785 eV), where the simulated XMCD signal has much less amplitude, but also in the L_2 (792–797 eV), where now an XMCD signal is calculated while it is practically absent in the experiment. Using the XMCD sum rule,²² we can relate these discrepancies also directly to the fact that the d_0 *ansatz* essentially does not carry an orbital moment.

The success of the cluster method for the analysis of both the high-energy spectroscopies and the ground-state magnetic moments provides confidence for its use to investigate the magnetocrystalline anisotropy in this material. We have

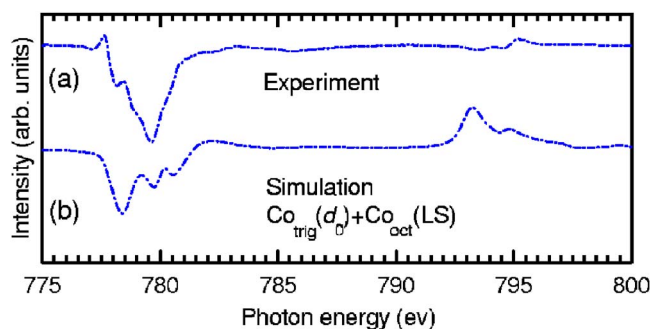


FIG. 3. (Color online) (a) Measured soft-x-ray magnetic circular dichroism spectrum (XMCD, $\mu^+ - \mu^-$); (b) simulated XMCD spectrum assuming a doubly occupied d_0 orbital for the Co_{trig} and low-spin (LS) Co_{oct} ions.

calculated the total energy of the $\text{Co}_{\text{trig}}\text{O}_6$ cluster as a function of the exchange field H_{ex} , directed either along the z axis (the c axis or the one-dimensional chain) or along the x axis (perpendicular to the c axis). The results for the d_2 *ansatz* are plotted in the left-hand panel of Fig. 4. It is evident that the lowest state gains energy when H_{ex} is along z and very little to nothing for H_{ex} along x . This demonstrates directly that the magnetocrystalline anisotropy should be large and directed along the z , consistent with the experimental observation that the magnetization parallel to c is almost sixfold of the one perpendicular to c (at 12 K and 5.5 T)³ and with the Ising nature of the magnetism. We note that the lowest curve in the figure shows an energy gain with a rate twice that of H_{ex} (along z), meaning that S_z is close to $2\mu_B$, which in turn is consistent with the HS ($S=2$) nature of the Co_{trig} ion.

We have also analyzed the magnetocrystalline anisotropy of the $\text{Co}_{\text{trig}}\text{O}_6$ cluster using the d_0 *ansatz*. The right-hand panel of Fig. 4 reveals that the total energy decreases for both directions of H_{ex} , but now with the important distinction that the energy for H_{ex} along x is always lower than for H_{ex} along z . This implies that the easy-magnetization axis should be perpendicular to the z axis, which is not consistent with the experimental facts. Also this contradiction thus effec-

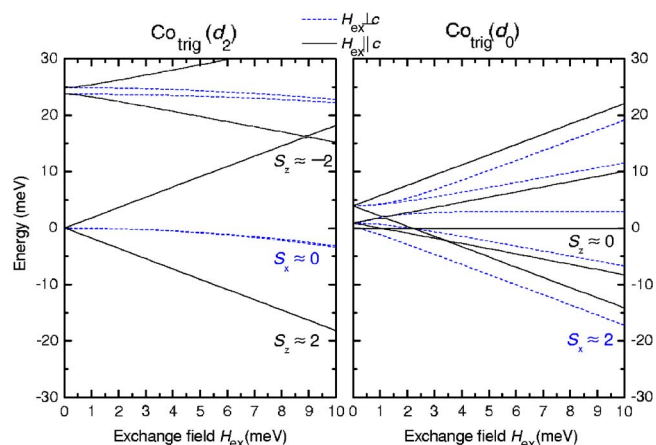


FIG. 4. (Color online) Total-energy level diagram for the Co_{trig} ion as a function of the exchange field H_{ex} along the z direction (c axis, solid black lines) and along the x direction (perpendicular to the c axis, dashed blue lines), with (left-hand panel) the d_2 and (right-hand panel) the d_0 orbital doubly occupied.

tively falsifies the d_0 *ansatz*.^{17,19}

To conclude, using soft x-ray absorption spectroscopy and the magnetic circular dichroism therein at the $\text{Co}-L_{2,3}$ edges we have experimentally determined that both Co ions in $\text{Ca}_3\text{Co}_2\text{O}_6$ are $3+$, with the Co_{trig} ion in the high-spin state and the Co_{oct} in the nonmagnetic state. The Co_{trig} ion carries an anomalously large orbital moment of $1.7\mu_B$ which we have been able to relate to the double occupation of the d_2 orbital. In addition, the detailed analysis of the spectral line shapes together with that of the magnetocrystalline anisotropy firmly establishes that the d_2 orbital lies lowest in energy¹⁸ and not the d_0 .^{17,19} This in turn also demonstrates that a proper incorporation of the spin-orbit interaction is required for the *ab initio* calculation of the delicate electronic structure of this material.

The authors are grateful to Hua Wu and Daniel Khomskii for stimulating discussions. The research in Köln was supported by the Deutsche Forschungsgemeinschaft (DFG) through SFB 608.

¹S. Aasland, H. Fjellvåg, and B. Hauback, *Solid State Commun.* **101**, 187 (1997).

²H. Kageyama, K. Yoshimura, K. Kosuge, H. Mitamura, and T. Goto, *J. Phys. Soc. Jpn.* **66**, 1607 (1997).

³H. Kageyama, K. Yoshimura, K. Kosuge, M. Azuma, M. Takano, H. Mitamura, and T. Goto, *J. Phys. Soc. Jpn.* **66**, 3996 (1997).

⁴A. Maignan, C. Michel, A. C. Masset, C. Martin, and B. Raveau, *Eur. Phys. J. B* **15**, 657 (2000).

⁵Y. B. Kudasov, *Phys. Rev. Lett.* **96**, 027212 (2006).

⁶V. Hardy, M. R. Lees, O. A. Petrenko, D. Mck. Paul, D. Flahaut, S. Hebert, and A. Maignan, *Phys. Rev. B* **70**, 064424 (2004).

⁷D. Flahaut, A. Maignan, S. Hébert, C. Martin, R. Retoux, and V. Hardy, *Phys. Rev. B* **70**, 094418 (2004).

⁸V. Hardy, D. Flahaut, M. R. Lees, and O. A. Petrenko, *Phys. Rev. B* **70**, 214439 (2004).

⁹O. Petrenko, J. Wooldridge, M. Lees, P. Manuel, and V. Hardy, *Eur. Phys. J. B* **47**, 79 (2005).

¹⁰H. Fjellvåg, E. Gulbrandsen, S. Aasland, A. Olsen, and B. C. Hauback, *J. Solid State Chem.* **124**, 190 (1996).

¹¹V. Hardy, S. Lambert, M. R. Lees, and D. Mck. Paul, *Phys. Rev. B* **68**, 014424 (2003).

¹²A. Maignan, V. Hardy, S. Hebert, M. Drillon, M. Lees, O. Petrenko, D. Mck. Paul, and D. Khomskii, *J. Mater. Chem.* **14**, 1231 (2004).

¹³R. Vidya, P. Ravindran, H. Fjellvåg, A. Kjekshus, and O. Eriksson, *Phys. Rev. Lett.* **91**, 186404 (2003).

¹⁴E. V. Sampathkumaran, N. Fujiwara, S. Rayaprol, P. K. Madhu, and Y. Uwatoko, *Phys. Rev. B* **70**, 014437 (2004).

¹⁵K. Takubo, T. Mizokawa, S. Hirata, J.-Y. Son, A. Fujimori, D. Topwal, D. D. Sarma, S. Rayaprol, and E.-V. Sampathkumaran,

- Phys. Rev. B **71**, 073406 (2005).
- ¹⁶V. Eyert, C. Laschinger, T. Kopp, and R. Frésard, Chem. Phys. Lett. **385**, 249 (2004).
- ¹⁷M.-H. Whangbo, D. Dai, H.-J. Koo, and S. Jobic, Solid State Commun. **125**, 413 (2003).
- ¹⁸Hua Wu, M. W. Haverkort, Z. Hu, D. I. Khomskii, and L. H. Tjeng, Phys. Rev. Lett. **95**, 186401 (2005).
- ¹⁹D. Dai and M.-H. Whangbo, Inorg. Chem. **44**, 4407 (2005).
- ²⁰Z. Hu, H. Wu, M. W. Haverkort, H. H. Hsieh, H. J. Lin, T. Lorenz, J. Baier, A. Reichl, I. Bonn, C. Felser *et al.*, Phys. Rev. Lett. **92**, 207402 (2004).
- ²¹C. Mitra, Z. Hu, P. Raychaudhuri, S. Wirth, S. I. Csiszar, H. H. Hsieh, H.-J. Lin, C. T. Chen, and L. H. Tjeng, Phys. Rev. B **67**, 092404 (2003).
- ²²B. T. Thole, P. Carra, F. Sette, and G. van der Laan, Phys. Rev. Lett. **68**, 1943 (1992).
- ²³T. Saitoh, T. Mizokawa, A. Fujimori, M. Abbate, Y. Takeda, and M. Takano, Phys. Rev. B **55**, 4257 (1997).
- ²⁴A. Tanaka and T. Jo, J. Phys. Soc. Jpn. **63**, 2788 (2004).
- ²⁵F. M. F. deGroot, J. Electron Spectrosc. Relat. Phenom. **67**, 529 (1994).
- ²⁶See the “Theo Thole Memorial Issue,” J. Electron Spectrosc. Relat. Phenom. **86**, 1 (1997).
- ²⁷T. Saitoh, A. E. Bocquet, T. Mizokawa, and A. Fujimori, Phys. Rev. B **52**, 7934 (1995).
- ²⁸Z. Hu, C. Mazumdar, G. Kaindl, F. M. F. de Groot, S. A. Warda, and D. Reinen, Chem. Phys. Lett. **297**, 321 (1998).
- ²⁹J. B. Goodenough, in *Progress in Solid State Chemistry*, edited by H. Reiss (Pergamon, Oxford, 1965), Vol. 5, p. 145.
- ³⁰P. G. Radaelli and S.-W. Cheong, Phys. Rev. B **66**, 094408 (2002).
- ³¹A. E. Bocquet, T. Mizokawa, K. Morikawa, A. Fujimori, S. R. Barman, K. Maiti, D. D. Sarma, Y. Tokura, and M. Onoda, Phys. Rev. B **53**, 1161 (1996).
- ³² $\Delta E_{d_2/d_0}^{\text{total}} = 0.102$ eV with an exchange field of $H_{\text{ex}} = 3$ meV, $H_{\text{ex}} \parallel c$.